[1] **Roberto San Jose**

[2] **J. L. Perez-Camanyo**

[3] **Miguel Jiménez Gañan**

Local impacts of global climate scenarios on biogenic CO2 fluxes

Abstract: - The objective of the research is to analyze the local impacts of various CMIP6 climate scenarios (SSP126, SSP245, SSP370 and SSP585) on biogenic CO2 emissions in five European regions from 2015 to 2050 using the WRF/Chem-VPRM tool. The study focuses on how climate change affects CO2 emissions from vegetation, with temperature increases leading to higher emissions due to increased plant respiration. Impacts vary by location and time, influenced by local vegetation and climate. This work is part of the European DISTENDER project, which integrates adaptation and mitigation strategies to address climate change risks.

Keywords: Climate change, CO2, biogenic emissions.

I. INTRODUCTION

Carbon dioxide (CO_2) is the main anthropogenic greenhouse gas contributing to climate change. Identifying CO_2 sources and sinks is crucial to mitigating global warming. Accurate emissions monitoring and forecasting tools are essential because CO_2 fluxes from vegetation can vary significantly by the meteorological conditions, introducing uncertainty. The capacity of ecosystems to absorb and release CO2 is influenced by various factors, including climate conditions such as temperature and radiation. Consequently, understanding the dynamics of CO2 uptake and release by terrestrial ecosystems is crucial for predicting future atmospheric CO2 levels and their potential effects on global warming [1].

While knowledge of the global carbon cycle has advanced, the identification of local CO2 sources and sinks remains limited. Quantifying CO2 exchange accurately poses challenges due to its spatial and temporal variability, particularly at the local scale. Regional variations in land-use patterns and emission sources lead to significant differences in CO2 fluxes, which are difficult to measure without specific climate data for each area [2]. Additionally, biogenic CO2 fluxes, which fluctuate with changing climatic conditions, contribute to the uncertainty in estimating local CO2 emissions [3]; [4]). While global climate models (GCMs) can provide general climate data, regional climate models (RCMs) can provide more detailed meteorological data, especially in complex terrain.

The most recent Intergovernmental Panel on Climate Change (IPCC) report emphasizes the need for high-resolution regional data and stresses the importance of downscaling GCMs with RCMs for accurate regional and urban analyses. Dynamic downscaling is an essential technique that provides high resolution climate data. This study uses the Weather Research and Forecasting (WRF) model to downscale CMIP6 data from five European regions to examine the impact of biogenic CO_2 fluxes in 2015-2050 climate scenarios. The WRF/Chem-VPRM model, which has proven effective in studying CO_2 fluxes, will focus on quantifying CO_2 sources and sinks. This research, part of the EU-funded DISTENDER project, aims to integrate adaptation and mitigation strategies to cope with the effects of climate change through participatory approaches. DISTENDER combines quantitative and qualitative analyses to explore interactions, synergies and trade-offs, with an emphasis on flexible and context-specific planning.

II. METHODOLOGY

2.1 Tools

[1] Environmental Software and Modelling Group, Computer Science School, Technical University of Madrid (UPM), Madrid, Spain. roberto@fi.upm.es

[2] Environmental Software and Modelling Group, Computer Science School, Technical University of Madrid (UPM), Madrid, Spain. jlperez@fi.upm.es

[3] Environmental Software and Modelling Group, Computer Science School, Technical University of Madrid (UPM), Madrid, Spain. m.jimenez@upm.es

Our study used the Weather Research and Forecasting (WRF) model, coupled to Chemistry version 4.5 (WRF-Chem) [5]. This Eulerian atmospheric transport model simulates the three-dimensional concentration of trace gases at each time step simultaneously with the meteorological fields in its passive tracer option. The WRF-Chem model was also coupled with the vegetation photosynthesis and respiration model (VPRM) [6], which calculates online biogenic CO_2 fluxes. The VPRM functions as a diagnostic parameterization tool for assessing vegetation CO_2 fluxes. It uses high-resolution land use data, vegetation indices derived from satellite observations, and simulated radiation and air temperature data from the WRF model. The accuracy of VPRM predictions can be affected by uncertainties in the input data. Previous research has shown that the variability of meteorological data influences the accuracy of model predictions more than land use and satellite data. The VPRM is capable of providing accurate simulations of CO_2 exchange processes between the biosphere and the atmosphere across large spatial and temporal scales.

VPRM is built around the concept of Net Ecosystem Exchange (NEE) of CO2, which represents the net flux of carbon dioxide between the land surface and the atmosphere. NEE is calculated as the difference between Gross Primary Production (GPP), the total amount of CO2 assimilated by plants during photosynthesis, and ecosystem respiration, the release of CO2 back into the atmosphere through biological processes. The mathematical formulation for NEE is given by Equation (1):

$$NEE = -GPP + Respiration \quad (1)$$

This equation highlights that NEE is negative when CO2 uptake (GPP) exceeds respiration, indicating that the ecosystem is acting as a carbon sink. Conversely, a positive NEE value indicates that the ecosystem is a net source of CO2.

The respiration component in VPRM is parameterized by Equation (2):

$$Respiration = \alpha\, T_{air} + \beta \quad (2)$$

α and β are respiration parameters. These parameters have been optimized specifically for European ecosystems, as described by Hilton et al. (2013). The dependency on air temperature reflects the temperature sensitivity of biological respiration processes, with higher temperatures generally leading to increased respiration rates. Tair is the air temperature.

Gross Primary Production (GPP) in VPRM is simulated using a combination of environmental and vegetation-specific parameters, as outlined in Equation (3):

$$GPP = (\lambda\, T_S W_s\, P_s)\, FAPAR_{PAV}\, \frac{1}{1+\frac{PAR}{PAR_0}}\, PAR \quad (3)$$

In this equation:

λ, represents the maximal light utilization efficiency, which is the ratio of CO2 assimilation to the photosynthetic photon flux density.

Ts, is the temperature sensitivity of photosynthesis, derived from air temperature.

Ws, denotes water stress, calculated from the Land Surface Water Index (LSWI),

Ps, represents the effect of leaf age on photosynthesis, also derived from LSWI, reflecting the seasonal variation in photosynthetic capacity.

$FAPAR_{PAV}$ is the fraction of absorbed photosynthetically active radiation, which correlates closely with the Enhanced Vegetation Index (EVI) derived from satellite data.

PAR is the photosynthetically active radiation, which is simulated from the shortwave radiation (SW) data provided by the WRF model, with the relationship $SW \approx 0.505 \times PAR$

PAR_0 is a reference value for PAR, representing the half-saturation point where photosynthesis is at half its maximum rate.

VPRM distinguishes between eight different vegetation types, each characterized by specific biosphere parameters, known as VPRM parameters.

EVI and LSWI are derived from MODIS surface reflectance data (MOD09A1, version 6) with a spatial resolution of 500 meters and a frequency of 8 days. Figure 1 shows the maximo EVI values fro 2018 year in the EURAF case study with 20 km of spatial resolution.

Anthropogenic CO_2 emissions were estimated using the EMIMO Emissions Model [7] based on the CAMS-GLOB-ANT emissions inventory, developed in the framework of the Copernicus Atmosphere Monitoring Service (CAMS), with a spatial resolution of 0.1x0.1 degree. The year 2018 serves as the reference year to isolate the climate signal. At each model time step, the VPRM reads temperature and downwelling shortwave radiation data from the WRF model to calculate biogenic CO2 fluxes, which are then transported and dispersed by the WRF/Chem model. This process requires wind and atmospheric turbulence parameters simulated by the WRF model.

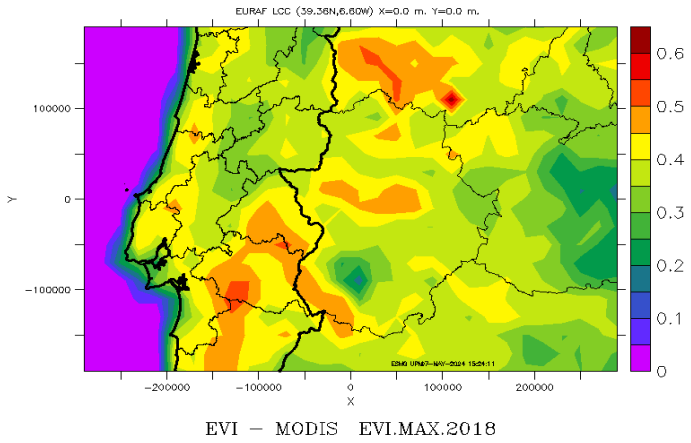

Figure 1. EURAF case study, map of the maximum EVI (0-1) for 2018 reference year.

Figure 1 shows that the EURAF case study area is a sparsely vegetated area with EVI values below 0.5, the highest EVI values are found in mountainous areas with some vegetation.

2.2 Experiment

The numerical modeling system simulates CO2 fluxes and atmospheric CO2 concentrations in five European regions as part of the DISTENDER project as is shown in Table 1.

Table 1: Case studies.

Identifier	Case study
Austria	Federal Ministry for Climate Protection, Environment, Energy, Mobility, Innovation and Technology (BMK)
HUAS	North-east of the Netherlands the Netherland Water Management Authority represented by Hanze University
EURAF	South-West Iberian Peninsula, Dehesa-Montado represented by European Agroforestry Federation
CMTo	Metropolitan City of Turin in Italy
Guimaraes	City in Portugal

Using a bidirectional nesting technique across multiple domains, the simulations span from 2015 to 2050, with 33 vertical layers and hourly outputs generated over 35 years for four climate scenarios. The WRF/Chem-VPRM model is run continuously each year, with weather conditions updated every six hours from the MPI-ESM1-2-HR climate model. The MPI-ESM1.2-HR (Max Planck Institute Earth System Model version 1.2 at high resolution) was selected due to its advantageous features, making it particularly well-suited for predictive modeling and comprehensive climate impact assessments. This model has been recognized in the literature for its balanced radiation budget and its explicit adjustment of climate sensitivity, which provides a robust foundation for long-term

climate projections. One of the primary reasons for its selection is its balanced radiation budget, which is essential for accurately simulating energy exchanges between the Earth and space. This balance is crucial for ensuring the reliability of long-term climate simulations, particularly for predicting temperature changes and related climate phenomena. Another key feature of the MPI-ESM1.2-HR is its climate sensitivity, explicitly set at 3ºK. Climate sensitivity refers to the increase in equilibrium temperature associated with a doubling of atmospheric CO2 concentrations. A sensitivity of 3ºK aligns with the range considered likely by the Intergovernmental Panel on Climate Change (IPCC), ensuring that the model's projections are consistent with current scientific understanding. As detailed in Müller et al. (2018), the adjustment process ensures that the model responds to greenhouse gas forcing in a manner that accurately reflects observed climate behavior, enhancing its predictive capabilities. The MPI-ESM1.2-HR is configured with a horizontal grid spacing of approximately 100 km in the atmosphere and 40 km in the ocean. This resolution strikes a balance between computational efficiency and the need for detailed representation of climate processes. The 100 km atmospheric grid enables the model to capture large-scale weather patterns and climate dynamics, while the finer 40 km resolution in the ocean is particularly effective for resolving ocean currents and temperature gradients, both critical for precise climate simulations. The choice of grid spacing is based on extensive research and validation, as outlined in Mauritsen et al. (2019). MPI provides the necessary data, which are interpolated using the CMIP6-to-WRFInterim tool to align with the WRF grid for regional dynamic downscaling. Four global CMIP6 scenarios (SSP1-2.6, SSP2-4.5, SSP3-7.0, and SSP5-8.5) have been rescaled for these simulations [8]. A summary of the scenarios is presented below:

SSP1-2.6: Sustainability - Going Green. This scenario represents a world that follows a low forcing trajectory, with aggressive mitigation efforts aimed at sustainability and reduction of GHG emissions. It assumes global cooperation for environmental protection, renewable energy adoption and efficient land use. The SSP1-2.6 scenario is characterized by a peak in global emissions followed by a rapid decline, with the goal of limiting global warming to well below 2°C above pre-industrial levels.

SSP2-4.5: Medium trajectory. SSP2-4.5 represents a medium trajectory of future GHG emissions, in which the world follows a path of moderate socioeconomic development. This scenario assumes a balance between fossil fuel use and renewable energy adoption, with no extreme policy changes. It represents a middle ground in which neither large mitigation efforts nor uncontrolled emissions dominate, leading to a stabilization of radiative forcing at around 4.5 W/m² by 2100.

SSP3-7.0: Regional rivalry. This scenario is in the upper-middle range of future GHG emissions and is characterized by a world divided into regions with strong nationalistic tendencies and limited global cooperation. In the SSP3-7.0 scenario, economic development is uneven, with significant disparities between regions. Environmental protection is not a priority and dependence on fossil fuels remains high, leading to a substantial increase in GHG emissions and a radiative forcing of 7.0 W/m² in 2100.

SSP5-8.5: Fossil fuel-based development. SSP5-8.5 represents a high forcing scenario, in which the world follows a path of rapid economic growth driven by intensive use of fossil fuels. In this scenario, technological advances focus primarily on economic expansion rather than environmental sustainability. As a result, GHG emissions increase significantly, leading to a radiative forcing of 8.5 W/m² in 2100. This scenario assumes minimal mitigation efforts, leading to substantial global warming and associated climate impacts.

III. RESULTS

To isolate the climate impact, we created maps showing the average differences between each year (2019, 2020, ..., 2050) and the reference year 2018. These maps illustrate changes over time, where negative values indicate an improvement in fluxes (which can be positive for emissions or negative for removals), and positive values indicate a decrease, either due to an increase in emissions or a decrease in removals. The following images ilustre the results of this study.

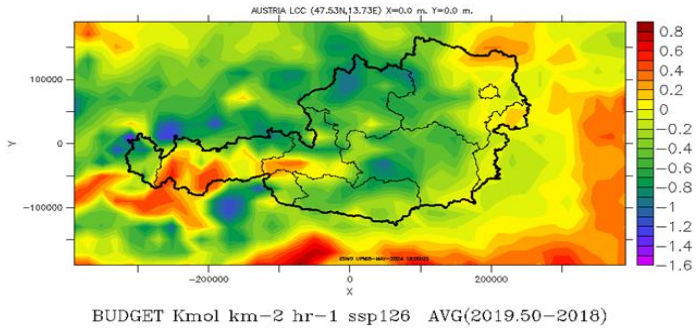

Figure 2. Austria case study, map of the BUDGET (Km km-2 hr-1) average differences between 2019 to 2050 minus 2018 for the SSP126 scenario.

Figure 2 shows the different trends in biogenic CO_2 fluxes between western and eastern regions. In the western regions, increasing temperatures exacerbate fluxes, leading to increased emissions or reduced CO_2 uptake and consequently raising atmospheric CO_2 levels. In contrast, eastern regions show modest improvements in fluxes, especially between 2040 and 2050.

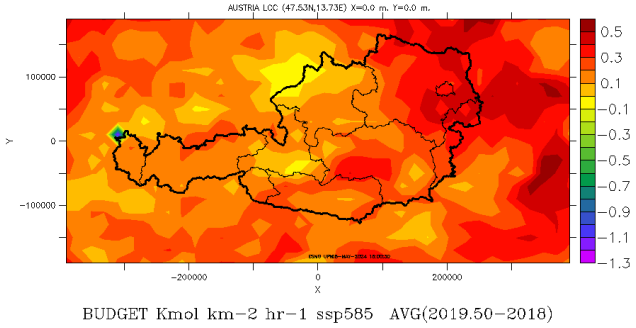

Figure 3. Austria case study, map of the BUDGET (Km km-2 hr-1) average differences between 2019 to 2050 minus 2018 for the SSP585scenario.

However, these improvements are not sufficient to counteract the deteriorating trends observed in the West, underscoring the need for targeted regional mitigation strategies. The analysis from 2019 to 2050 reveals a worsening trend in western fluxes due to persistent temperature increase, while eastern regions, despite showing some resilience, are unable to fully mitigate the impacts observed in western areas. In figure 3 we can see a general deterioration of CO2 biogenic fluxes with the scenario SSP585 over the same area (Austria).

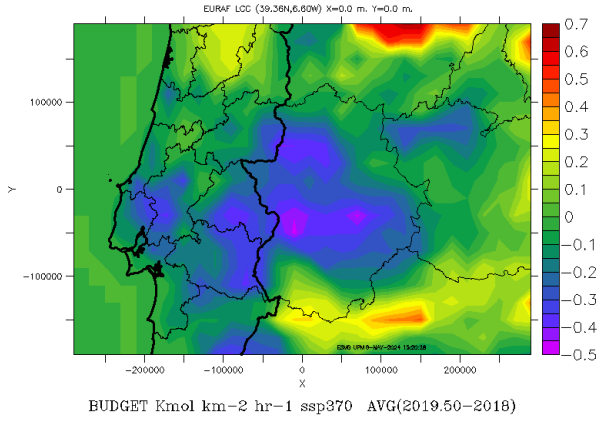

Figure 4. EURAF case study, map of the BUDGET (Km km-2 hr-1) average differences between 2019 to 2050 minus 2018 for the SSP370 scenario.

Figure 4 illustrates the impact of the SSP370 scenario on biogenic CO_2 fluxes, revealing improvements attributed to lower temperatures that increase CO_2 uptake by vegetation through more efficient photosynthesis and respiration.

Despite these improvements in fluxes, CO_2 concentrations show only minor changes, suggesting that other factors, such as anthropogenic emissions and atmospheric transport, also play an important role. The increase in biogenic fluxes in the SSP370 scenario underlines the climate mitigation potential of natural systems, but the minimal changes in CO_2 concentrations highlight the complexity of the carbon cycle. Temporal analysis within the SSP370 scenario shows stable improvements in biogenic fluxes, indicating that sustained carbon uptake is likely if favorable conditions continue.

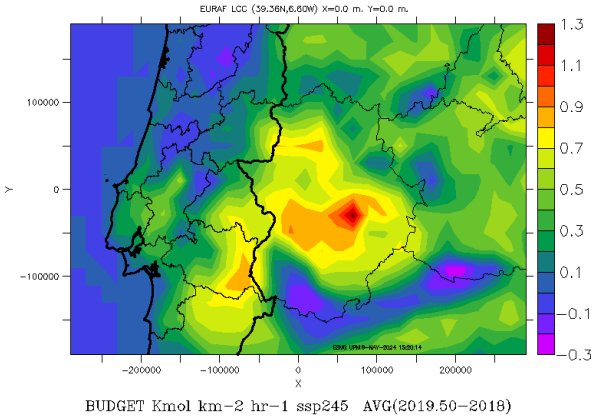

Figure 5. EURAF case study, map of the BUDGET (Km km-2 hr-1) average differences between 2019 to 2050 minus 2018 for the SSP245 scenario.

Figure 5 on the SSP245 scenario illustrates a worsening situation for biogenic CO2 fluxes. The main area of deterioration is concentrated in the central region of the domain, which coincides with the regions where temperatures are projected to increase. Rising temperatures in this central region are likely to contribute to increased biogenic CO2 emissions, as warmer conditions tend to accelerate processes such as plant respiration, releasing more CO2 into the atmosphere. This highlights a critical feedback mechanism, whereby increasing temperatures exacerbate CO2 fluxes, further contributing to climate change impacts in this area.

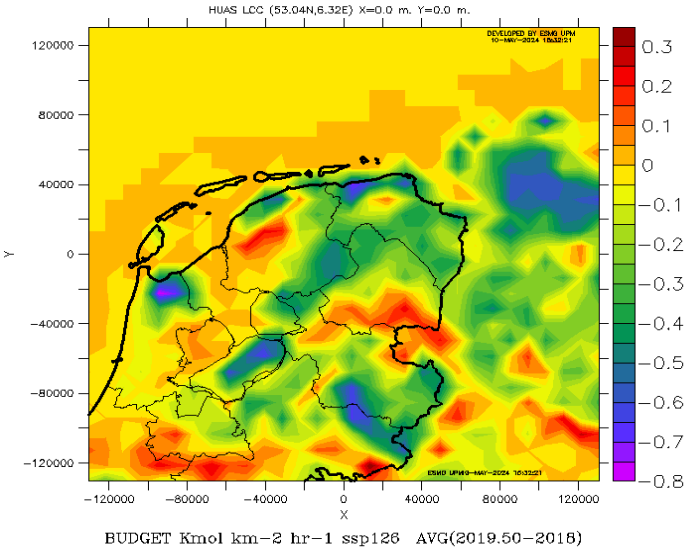

Figure 6. HUAS case study, map of the BUDGET (Km km-2 hr-1) average differences between 2019 to 2050 minus 2018 for the SSP126 scenario.

Figure 6 illustrates the varied impact of the SSP126 scenario on biogenic fluxes and CO_2 concentrations in different regions. The spatial distribution highlights both positive and negative effects, reflecting varying responses to climatic factors such as temperature, precipitation and vegetation dynamics. Regions with favorable conditions experience marked improvements in biogenic fluxes, leading to increased carbon uptake and reduced CO_2 concentrations, demonstrating the benefits of low-emission pathways. In contrast, areas facing adverse conditions

show worsening fluxes, underscoring the need for tailored climate strategies. While SSP126 indicates generally positive trends, targeted interventions are crucial to address specific regional challenges and ensure effective climate resilience and mitigation.

Figure 7 illustrates the results of the SSP585 scenario, which foresees a significant intensification of biogenic CO2 emissions. The worsening of biogenic CO2 emissions in this scenario is mainly due to rising local temperatures, which accelerate natural processes such as plant respiration.

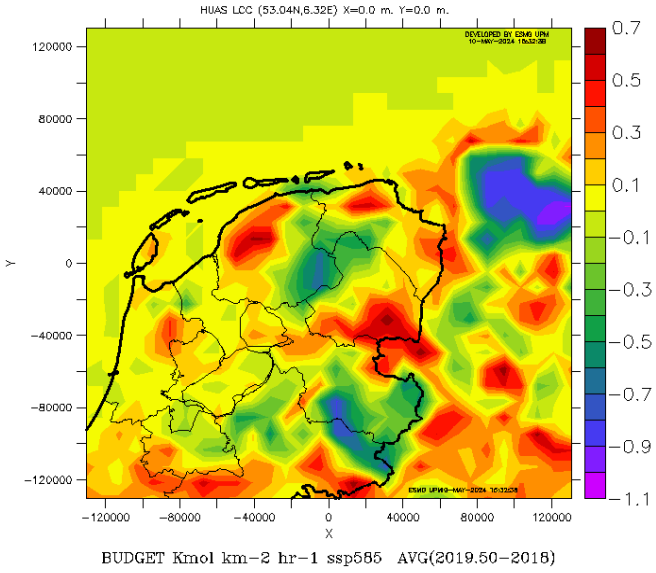

Figure 7. HUAS case study, map of the BUDGET (Km km-2 hr-1) average differences between 2019 to 2050 minus 2018 for the SSP585 scenario.

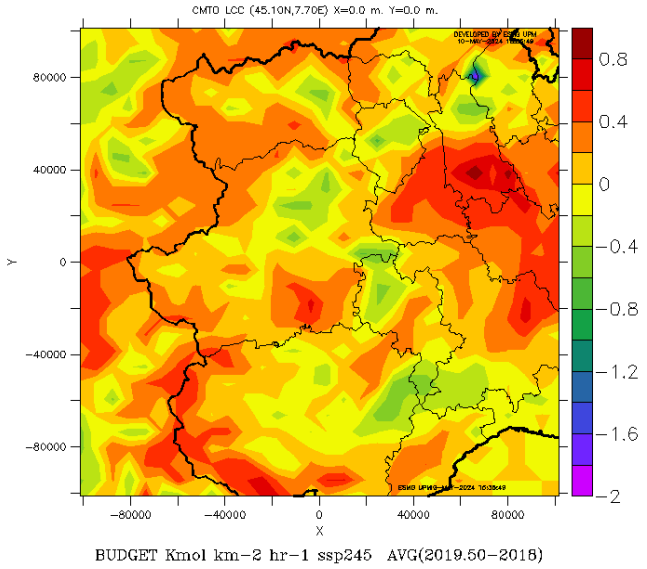

Figure 8. CMTo case study, map of the BUDGET (Km km-2 hr-1) average differences between 2019 to 2050 minus 2018 for the SSP245 scenario.

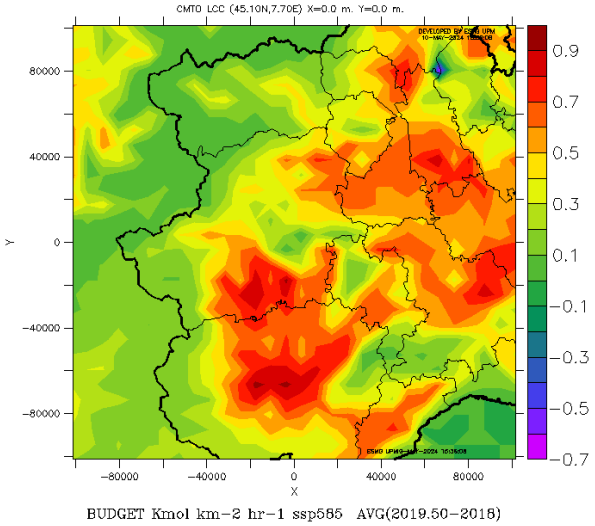

Figure 9. CMTo case study, map of the BUDGET (Km km-2 hr-1) average differences between 2019 to 2050 minus 2018 for the SSP585 scenario.

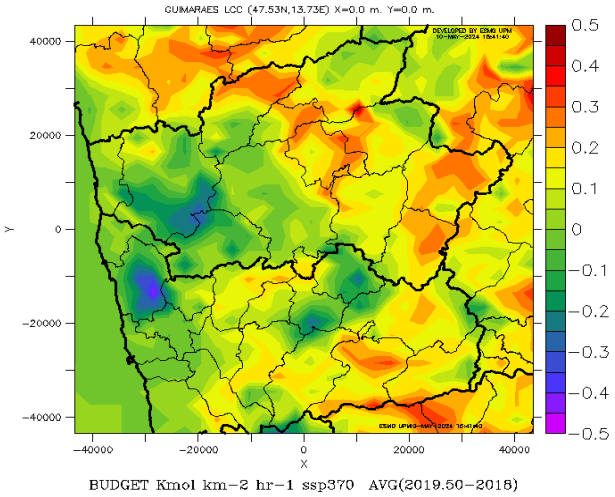

Figure 10. Guimaraes case study, map of the BUDGET (Km km-2 hr-1) average differences between 2019 to 2050 minus 2018 for the SSP370 scenario. 3 km spatial resolution.

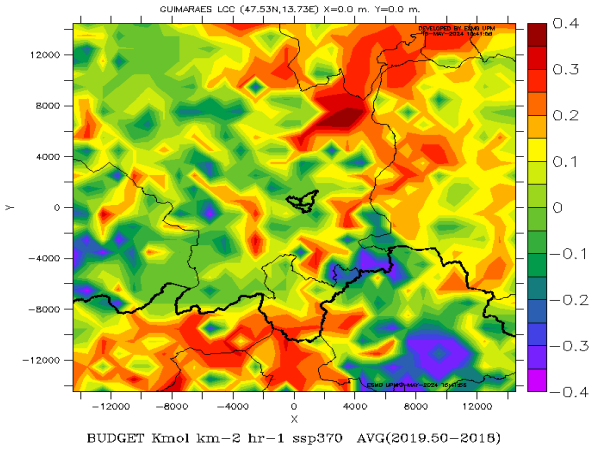

Figure 11. Guimaraes study, map of the BUDGET (Km km-2 hr-1) average differences between 2019 to 2050 minus 2018 for the SSP370 scenario. 1 km spatial resolution.

Figure 8 and Figure 9 general increase in biogenic CO_2 fluxes for sceanrios SSP245 and SSP585 throughout the study area, reflecting increased emissions or reduced uptake by vegetation under future scenarios influenced by adverse climatic conditions, such as increasing temperatures and changing precipitation patterns. Despite this overall negative trend, some areas show improvements in biogenic fluxes, probably due to localized factors such as microclimates or resilient vegetation. In particular, the eastern region of Turin experiences significant increases in CO_2 concentrations and air temperatures, indicating a marked reduction in carbon sequestration capacity. These results underline the need for specific climate strategies, especially in regions such as eastern Turin, to effectively address the challenges of deteriorating biogenic fluxes and rising CO_2 levels.

Figure 10 and 11 show minimal changes in biogenic CO_2 emission fluxes and air temperature, with a slight decrease in CO_2 concentrations. Figure 10 is the map with 3 kilometers of spatial resolution and Figure 11 with 1 km of spatial resolution, the results are coherent between domains. The small variations in biogenic fluxes indicate that vegetation and land management practices in the region effectively maintain a stable balance between carbon uptake and emissions, even in the midst of climatic fluctuations. This stability may be due to adaptive vegetation types or successful land management strategies that help mitigate the effects of climate change.

IV. CONCLUSIONS

We employed a dynamic downscaling tool, WRF/Chem-VPRM-EMIMO, to analyze the impacts of future climate scenarios on vegetation CO_2 emission fluxes, air temperature and CO_2 concentrations in five European regions. Four global climate scenarios - SSP126, SSP245, SSP370 and SSP585 - modeled by the global climate model MPI-ESM1.2-HR, were rescaled for the period 2015-2050. To isolate the effects of climate change, we used the 2018 anthropogenic emissions inventory, land use types and satellite data as reference. An overall increase in temperature was observed in all scenarios and case studies, with the most significant increases predicted in the CMTo region and the smallest in HUAS. Interestingly, the SSP3 scenario showed temperature decreases in Austria, EURAF and GUIMARAES. Temperature increases led to increased CO_2 emissions from vegetation, as warmer temperatures favor plant respiration. Impacts on biogenic CO_2 emission fluxes varied significantly between regions and epochs, reflecting the strong influence of existing vegetation patterns. CO_2 concentrations tended to increase in Austria, EURAF and CMTo, with the most substantial increases expected in these regions, while slight decreases were observed in HUAS and GUIMARAES. Despite improvements in biogenic emission fluxes in some areas, CO_2 concentrations continued to increase due to the influence of boundary conditions and CO_2 transport mechanisms.

These results highlight the variability of local climate impacts and demonstrate that the effects of global climate scenarios can differ significantly depending on location. This highlights the importance of regional studies in understanding and addressing climate change impacts.

V. ACKNOWLEDGEMENTS

The UPM authors acknowledge the computer resources and technical assistance provided by the Centro de Supercomputación y Visualización de Madrid (CeSViMa). The UPM authors thankfully acknowledge the computer resources, technical expertise and assistance provided by the Red Española de Supercomputación. DISTENDER has received funding from the European Union's Horizon EU research and innovation programme under grant agreement No 101056836".

REFERENCES

[1] Baldocchi, Dennis, et al. "Terrestrial Carbon Cycle Variability." F1000Research, vol. 5, 26 Sept. 2016, p. 2371, https://doi.org/10.12688/f1000research.8962.1.

[2] Bezyk, Yaroslav, et al. "Assessment of Urban CO2 Budget: Anthropogenic and Biogenic Inputs." Urban Climate, vol. 39, Sept. 2021, p. 100949, https://doi.org/10.1016/j.uclim.2021.100949. Accessed 1 May 2022.

[3] Lei, Na, and Jichang Han. "Effect of Precipitation on Respiration of Different Reconstructed Soils." Scientific Reports, vol. 10, 30 Apr. 2020, p. 7328, www.ncbi.nlm.nih.gov/pmc/articles/PMC7193616/, https://doi.org/10.1038/s41598-020-63420-x. Accessed 22 Nov. 2021.

[4] McHale, Melissa R., et al. "Carbon Lost and Carbon Gained: A Study of Vegetation and Carbon Trade-Offs among Diverse Land Uses in Phoenix, Arizona." Ecological Applications, vol. 27, no. 2, Mar. 2017, pp. 644–661, https://doi.org/10.1002/
eap.1472. Accessed 16 Apr. 2020.

[5] Grell, Georg A., et al. “Fully Coupled ‘Online’ Chemistry within the WRF Model.” Atmospheric Environment, vol. 39, no. 37, Dec. 2005, pp. 6957–6975, doi:10.1016/j.atmosenv.2005.04.027.

[6] Mahadevan, Pathmathevan, et al. “A Satellite-Based Biosphere Parameterization for Net Ecosystem CO2exchange: Vegetation Photosynthesis and Respiration Model (VPRM).” Global Biogeochemical Cycles, vol. 22, no. 2, 12 Apr. 2008, p. n/a-n/a, https://doi.org/10.1029/2006gb002735. Accessed 21 July 2021.

[7] R. San José, et al. “Sensitivity of Feedback Effects in CBMZ/MOSAIC Chemical Mechanism.” Atmospheric Environment, vol. 115, 1 Aug. 2015, pp. 646–656, https://doi.org/10.1016/j.atmosenv.2015.04.030. Accessed 19 May 2023.

[8] O’Neill, Brian C., et al. “The Scenario Model Intercomparison Project (ScenarioMIP) for CMIP6.” Geoscientific Model Development, vol. 9, no. 9, 28 Sept. 2016, pp. 3461–3482, pure.iiasa.ac.at/13868/1/The%20Scenario%20Model%20Intercomparison%20P oject%20%28ScenarioMIP%29%20for%20CMIP6.pdf, https://doi.org/10.5194/gmd-9-3461-2016.